

An investigation of the electronic properties of MgO doped with group III, IV, and V elements:
trends with varying dopant atomic number

This article has been downloaded from IOPscience. Please scroll down to see the full text article.

2010 J. Phys.: Condens. Matter 22 046002

(<http://iopscience.iop.org/0953-8984/22/4/046002>)

View [the table of contents for this issue](#), or go to the [journal homepage](#) for more

Download details:

IP Address: 129.252.86.83

The article was downloaded on 30/05/2010 at 06:39

Please note that [terms and conditions apply](#).

An investigation of the electronic properties of MgO doped with group III, IV, and V elements: trends with varying dopant atomic number

Guodong Liu, Shulin Ji, Liangliang Yin, Guangtao Fei and Changhui Ye¹

Key Laboratory of Materials Physics and Anhui Key Laboratory of Nanomaterials and Technology, Institute of Solid State Physics, Chinese Academy of Sciences, Hefei 230031, People's Republic of China

E-mail: chye@issp.ac.cn

Received 28 September 2009, in final form 29 November 2009

Published 5 January 2010

Online at stacks.iop.org/JPhysCM/22/046002

Abstract

The electronic properties and the trends with varying dopant atomic number of III, IV, and V main group elements in MgO have been investigated using density functional theory. It is found that all of the geometry-optimized systems with the dopant atom replacing O in MgO exhibit half-metallic ferromagnetic properties regardless of metal or non-metal doping, and this agrees well with other theoretical computations. However, because of the high formation energy of metal atoms substituting for O atoms, we have calculated metal atom substitution for the Mg atom in MgO. We found that this system has a paramagnetic state and the formation energy is much lower than that of the former case. Finally, we have performed calculations for MgO doped with an F atom which shows a metallic behavior.

1. Introduction

Half-metallic ferromagnetism has attracted particular interest in spintronics, since there is only one electronic channel at the Fermi level and therefore nearly 100% spin polarization. Recently, scientific interest has been focused on the d^0 magnetic half-metal system, in which the interactions of p states play an important role in forming this property. To look for this d^0 magnetic half-metal material, many researchers have theoretically investigated monoxide materials. Elfimov *et al* studied Ca vacancies in CaO using model Hamiltonian and *ab initio* band structure methods, and proposed that such a system had ferromagnetic ground states with small local magnetic moments, which were due to a kind of molecular Hund's rule coupling with energetics determined by kinetic energy and symmetry considerations rather than by exchange interactions [1]. Osorio-Guillén *et al* [2] further pointed out that one cannot obtain more than 0.003% Ca vacancies at equilibrium conditions because of the high

formation energy for vacancies even under the most favorable growth conditions. Similar to Ca vacancies in CaO, MgO with intrinsic Mg vacancies also displayed half-metallic ferromagnetism [3]. Elfimov *et al* theoretically predicted a new diluted ferromagnetic semiconductor of the N-doped SrO system, and gave an experimental verification in 2007 [4]. However, Kenmochi *et al* [5] did not find finite magnetic moment in CaO with Ca vacancies by using the Korringa–Kohn–Rostoker coherent potential approximation with local spin density approximation (KKR-CPA-LSDA) method that allows magnetic disorder to be taken into account. They also calculated B-, C-, and N-doped CaO systems using the same method, and found that B, C, and N impurities showed finite local magnetic moments in CaO at the oxygen substitutional site. Moreover, these C- and N-doped CaO exhibited room-temperature ferromagnetism with half-metallic density of states. Because of the same cubic rocksalt structure, B-, C-, or N-doped MgO may have similar properties to non-metal doped CaO. Recently, Bulut [6], Dinh [7], and Bannikov [8] groups have reported results for non-metal doped

¹ Author to whom any correspondence should be addressed.

MgO similar to those for doped CaO, although they used different calculation methods. Pardo *et al* [9] further studied the substitutional N in the alkaline earth monoxide series MgO, CaO, SrO, and BaO in detail by using an augmented plane wave plus local orbitals (APW + lo) method. It was found that greater delocalization was permitted and the band gap was reduced as the cationic radius was increased ($U_{\text{eff}} = 5.5$ eV). The magnetic coupling decreased rapidly as the value of U increased. In fact, the effect of such non-metal doping is similar to that of the cation vacancies in MgO or CaO. For such systems, the mechanism is different from the known transition metal doping in oxide semiconductors, where d states play an important role in forming ferromagnetism. The exact mechanism for such d^0 half-metallic ferromagnetism continues to be strongly debated in the literature.

Currently, much of the experiment work focuses on transition metal doped MgO, for example, Narayan *et al* produced Ni-doped MgO crystals using an arc fusion technique and found a paramagnetic property at dopant concentrations of 0.5% and 4% in the absence of defects or charge carriers [10], and Dutta *et al* synthesized 10% Cu-doped MgO by the incipient wetness impregnation technique and found that it was also paramagnetic [11].

In this work, we have systematically investigated the electronic structures and the magnetism of MgO doped with III, IV, V main group elements (both metal and non-metal elements) under a concentration of 25%. We have investigated the first case, in which dopant atoms replace the O atom; then we have calculated the situation with metal atom substitution for the Mg atom; finally we have studied an F-doped MgO system.

2. Computational details

In this paper, a model was constructed using the $\text{Mg}_4\text{O}_3\text{X}$ cell for all the impurity atoms and the Mg_3XO_4 cell for metal atom substitution for Mg. We used the spin-polarized density functional theory (DFT) which was performed using the plane-wave ultrasoft pseudopotential method [12] implemented in CASTEP [13] to carry out the calculation of geometry optimization and electronic structures. The exchange–correlation interaction was treated with the generalized gradient approximation (GGA) using the Perdew–Burke–Ernzerhof (PBE) functional [14], and strong correlation effects were introduced by means of the LSDA + U scheme [15] by introducing effective U for oxygen and impurity np ($n = 2, 3,$ and 4 , the outmost p shell) states to reduce the magnetic coupling. To further localize the moments, U_{eff} was taken as 5.5 eV [16]. A plane-wave cutoff was taken as 380 eV. The Brillouin zone integration was performed within the Monkhorst–Pack scheme [17] using $6 \times 6 \times 6$ k points for the cells. The iteration was terminated until the total energy difference was less than 1.0×10^{-5} eV/atom and the maximal displacement of atoms was less than 1.0×10^{-3} Å. The 3d electrons of Ga, Ge, and As atoms were included in all computations. The on-site charge and the spin magnetic moments were evaluated via Mulliken population analysis [18]. It is well known that using the WIEN2k code

with a full-potential augmented plane wave (FLAPW), the magnetic moments can be calculated only inside the Muffin-tin spheres (as the difference between orbital populations with various spin orientations), and using CASTEP, the magnetic moments are evaluated by Mulliken formalism for pseudoatomic orbitals. Therefore, the magnetic moments estimated by the CASTEP method usually turn out to be higher than those in FLAPW; however, it had little effect on the trends we studied.

3. Results and discussions

MgO has the rocksalt crystal structure with a lattice constant of 4.213 Å [19], and is a nonmagnetic insulator with a forbidden gap of 7.809 eV [20]. The valence-band maximum of MgO is mainly contributed by O 2p state, and Mg 3s state constitutes the bottom of the conduction band. When III, IV, and V main group atoms substitute for O or Mg in the lattice sites, the number of total electrons in the system decreases or increases, leading to the movement of the Fermi level towards the valence band or conduction band, and the system is no longer an insulator. Here, we do not consider the Jahn–Teller effect which does not affect the trends we investigate, just as Pardo *et al* [9] pointed out that the atomic relaxations had little effect on the localization of the magnetic moment and the magnetic coupling.

3.1. MgO doped with III, IV, V main group elements (both metal and non-metal elements)

The impurity-induced polarization of the host electron spins is characterized by the density of states (DOS) spectra shown in figure 1. Because of the deep level of d electron states (not shown here), they have no effects on the electron behavior and magnetism in such systems. We first consider the electronic structure of MgO systems doped with main group III atoms (B, Al, and Ga), the DOS and projected DOS (PDOS) for separate spin directions are shown in figure 1(a). The spectra of all the three doped systems exhibit a metallic character for the spin-up channel and have a forbidden band (band gap) for carriers with the spin-down channel, which is different from other papers [8, 21]. Actually, from the density of spin-polarized states of B-doped MgO by Bannikov *et al* [8] it was difficult to identify which spin channel was conductive because the Fermi level approached closer to the spin-up band from the DOS figure due to B doping. Although Al and Ga atoms are metal elements, they also display the same property as non-metal B-doped MgO because these elements have a similar valence-electron configuration and similar valence-electron behavior in MgO. For MgO doped with IV (C, Si, and Ge) and V (N, P, and As) group atoms, it also displays spin polarization and metallic character in the spin-down direction (figures 1(b) and (c)). Such a half-metallic state formed because of a spontaneous spin polarization of electron states in the np bands of dopant atoms. These results are in agreement with other work [6–8, 21], although the computational methods are rather different. In addition, as seen from figure 1, the spin splitting near the Fermi level mainly comes from the substitutional

Table 1. III, IV, V main groups and O, F atoms' outermost shell orbital energies. (Adopted from: [23]).

III			IV			V			VI	VII
B	Al	Ga	C	Si	Ge	N	P	As	O	F
-8.56	-5.80	-5.76	-11.24	-7.00	-7.44	-14.05	-9.69	-9.12	-17.03	-20.17

atoms' np states regardless of metal or non-metal doping, and the extent of spin splitting gets weaker with the order of the doping of the III \rightarrow IV \rightarrow V main group atoms because the energy difference $\Delta\varepsilon$ (O2p-Xnp) decreases ($\varepsilon_{B2p} = -8.56$ eV, $\varepsilon_{C2p} = -11.24$ eV, $\varepsilon_{N2p} = -14.05$ eV, $\varepsilon_{O2p} = -17.03$ eV, as listed in table 1) and the electron density grows in this series. The dopant np band shifts towards lower energies and leads to a decrease in the $np\uparrow$ - $np\downarrow$ splitting with the minimum for the np orbital of the atoms doped with main group V.

Considering that electron states on the Fermi level lead to a large ferromagnetic (FM) coupling and the electron states get larger with increase of the atomic number of the dopant atoms in the same group, we can conclude that MgO doped with main group V atoms has the maximum electron states on the Fermi level. By using the pseudopotential-like self-interaction corrected local spin density method Dinh *et al* [7] predicted that the Curie temperature of C- and N-doped (25%) CaO was as high as room temperature.

3.2. Only metal atoms substituting Mg atoms

The electron behavior is different from that of the first case. As expected, one Al or Ga dopant induces one more electron and one Ge dopant induces two more electrons. The DOS and the PDOS of these metallic atom doped MgO are shown in figures 2(a) and (b) (here we did not list the DOS of Ga-doped MgO which is similar to that of Al-doped MgO; while we listed the DOS of pure MgO in figure 2 for convenience of comparison, using the DOS of MgO as a reference), and it can be seen that all of them did not reveal spin polarization and the dopant atoms did not change the shape of the PDOS on the Mg atom (the PDOS of the Mg atom is not shown here) with only a parallel move of levels to the low energy level (~ 5 eV). An electronic structure calculation for Al-doped MgO gave a paramagnetic state, and the Fermi level moved to high levels and entered the conduction band (figure 2(a)). The additional electron, contributed by the Al atom, formed impurity levels in the band gap. The width of the p orbital of the O atom (~ 6.7 eV) became more delocalized compared with the PDOS on the O atom in figure 2(c). When the Ga atom was doped, although it has 3d electrons, the results showed that the d electron states localized at a very deep level and made no difference to the electron behavior and magnetism in the system. The electronic structure of Ga-doped MgO is similar to that of Al-doped MgO and its ground state is also paramagnetic. However, when the Ge atom was doped in MgO, the electron structure was rather different from that of the Ga-doped system. The Ge 3d electrons did not affect the magnetic behavior, either. Our calculation gave a paramagnetic ground state of the Ge-doped MgO, as seen from figure 2(b). This system was calculated as a semiconductor with a band gap of 0.702 eV, and the two extra electrons formed an energy

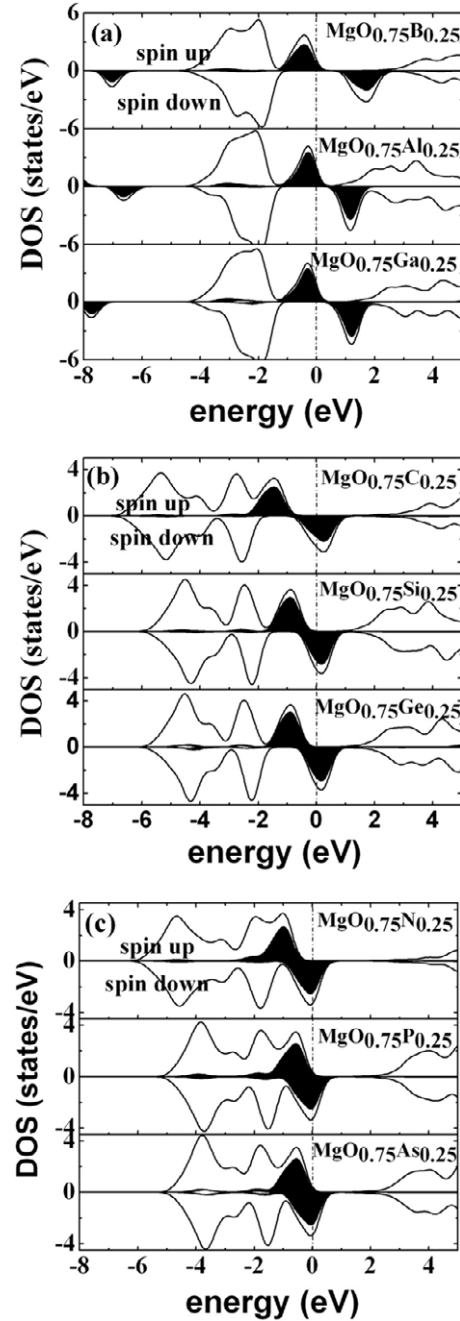


Figure 1. Total DOS (solid) and the projected DOS on the impurity atoms' outermost p states (shaded) for MgO doped with III, IV, V main group atoms, shown in (a)–(c), respectively.

band at the top of the valence band. Further analysis (figure 3) indicates that the outermost shell p orbitals of O and Ge atoms have moderate coupling near the Fermi level because of the similarity of the PDOSs (we expanded the outermost shell p electron states of the Ge atom ten times for clarity), and such coupling makes the two extra electrons occupy the valence

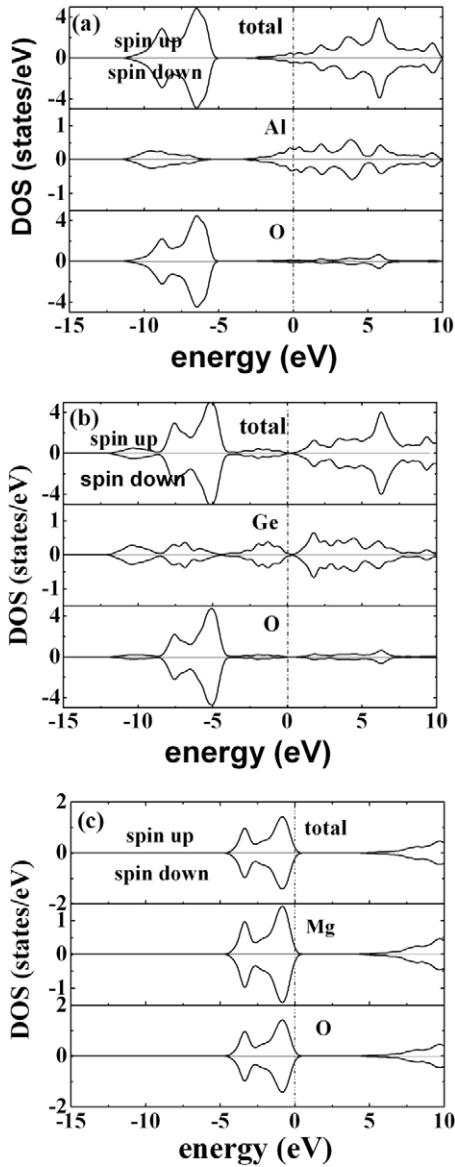


Figure 2. The density of states of Mg_3AlO_4 and Mg_3GeO_4 are shown in (a) and (b); from up to down is the total DOS, and the projected DOS on impurity and O atoms; the densities of states of MgO are shown in (c); from up to down is total DOS, and projected DOS on Mg and O atoms.

band, instead of the conduction band. Considering that there is no such coupling in Al- and Ga-doped MgO, the electron behavior of these doped systems has a close relationship with the valence-electronic configuration of impurity atoms.

3.3. Magnetic moments, spin polarization energy, and so on of the $\text{Mg}_4\text{O}_3\text{X}$ systems

According to our calculations, all of the $\text{Mg}_4\text{O}_3\text{X}$ systems displayed spontaneous magnetization and represented half-metal ferromagnetism. The numerical values of magnetic moments (MM) on atoms, geometry-optimized lattice constant (a (Å)), formation energy per unit cell (E_f), and the band gap of one spin channel (E_g) are listed in table 2 for MgO doped with III, IV, and V main group atoms, respectively.

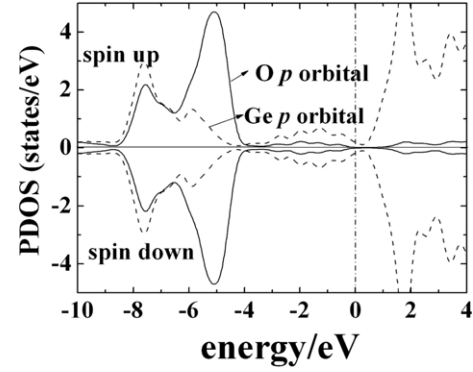


Figure 3. The projected DOS on the outermost p electrons of O and Ge atoms in Mg_3GeO_4 . (The projected DOS on Ge p states is enlarged ten times.)

Firstly, the lattice constant of the doped system increases with dopant atomic number, since the bigger the radius of the dopant atoms, the larger the lattice constant; the impurity hole state becomes more delocalized and the band gap simultaneously decreases for the same main group. Secondly, for the same main group atom dopants, upon increasing the lattice constant by introducing a bigger impurity atom, the MM on the impurity atom gets smaller, which is determined by the tendency of the impurity hole state. While different main group dopant atoms have an effect on the MM, III main group element doped MgO have the maximal MM per cell and on the impurity atoms. For example, according to our calculation results, the MM on a B atom is $2.62 \mu_B$, about 2.79 times that on an N atom, and 1.39 times that on a C atom, and MM of the B-doped MgO cell is three times that of an N-doped cell. In principle, we can show a qualitative explanation for it: the outermost shell electrons of Mg and dopant atoms are arranged following the Pauli exclusion principles and Hund rules, as shown in the schematic diagram in figure 4. According to the molecular orbital hybridization theory, for the B-doped situation, the system has three unpaired electrons, while for C and N, it has two and one, respectively. Therefore, the magnetic moment value on B should be three times that on N, and 1.5 times that on C, which agrees well with our calculation results. Thirdly, comparing the values of the formation energy in the table, E_f gets larger with the increase of dopant atomic number in the same main group. It reveals that MgO doped with N is most stable, which is consistent with the fact that the difference in atom radius between N and O is the smallest for V main group doping and the induced distortion of the lattice is the smallest. The numerical values of formation energy for the three metallic atoms Al, Ga, and Ge substituting for the Mg atom were calculated as 1.260 eV, 3.035 eV, and 3.213 eV, respectively, therefore it is a straightforward conclusion that metallic atom substitution for the O atom in MgO is less possible because of the much higher formation energy than in the substitution for the Mg atom. We define the spin polarization energy (ΔE) as the difference of the minimized total energy of the spin-polarized system (E^{LSDA}) and the minimized total energy of the non-spin-polarized (E^{LDA}) system: $\Delta E = E^{\text{LSDA}} - E^{\text{LDA}}$, as shown in figure 5, which is the quantification for the $2p\uparrow - 2p\downarrow$ splitting. Main group III atom dopants have the maximal

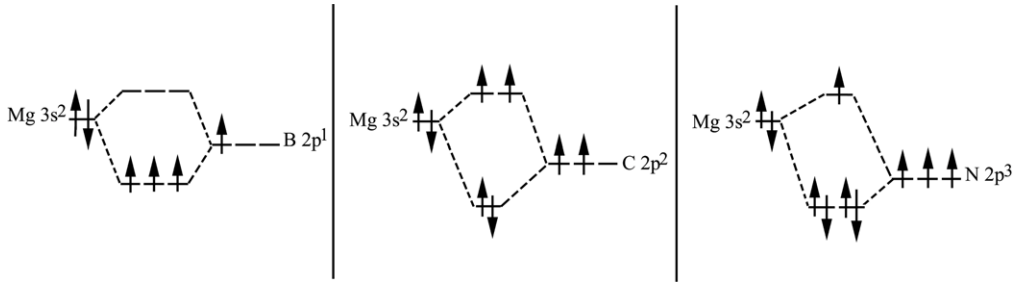


Figure 4. Schematic diagram of the outermost shell electrons of Mg and the arrangement of impurities (taking B, C, and N atoms as examples) on the p orbital.

Table 2. Crystallographic lattice constant (a (Å)), formation energy (E_f (eV unit⁻¹)), magnetic moments on atoms (μ_B per cell), and band gap width (E_g) for the spin-up channel (* this mark represents E_g for the spin-down channel) of MgO doped with III, IV, V main group atoms.

Main group atoms doped	Impurity systems	a (Å)	E_f (eV unit ⁻¹)	Magnetic moment (μ_B)			E_g (eV) (spin up)
				X	O	Cell	
III	MgO _{0.75} B _{0.25}	4.50	20.649	2.62	0.06	3.00	1.79*
	MgO _{0.75} Al _{0.25}	4.83	19.838	2.92	0.06	3.00	1.59*
	MgO _{0.75} Ga _{0.25}	4.78	20.935	2.62	0.10	3.00	1.24*
IV	MgO _{0.75} C _{0.25}	4.42	10.756	1.88	0.10	2.00	1.71
	MgO _{0.75} Si _{0.25}	4.76	12.006	1.80	0.14	2.00	0.84
	MgO _{0.75} Ge _{0.25}	4.78	12.148	1.72	0.16	2.00	0.54
V	MgO _{0.75} N _{0.25}	4.35	10.715	0.94	0.08	1.00	2.56
	MgO _{0.75} P _{0.25}	4.69	11.977	0.80	0.12	1.00	1.15
	MgO _{0.75} As _{0.25}	4.76	12.268	0.78	0.14	1.00	0.95

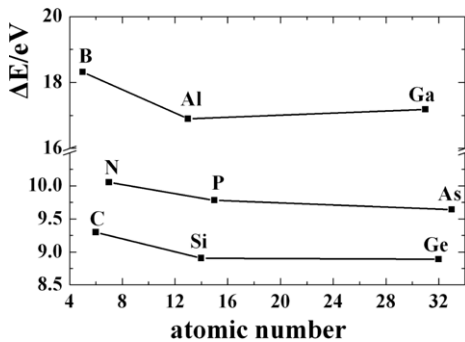


Figure 5. The spin polarization energy of MgO doped with different main group atoms.

value of spin polarization energy among these three main group atom dopants, which is due to the fact that MgO doped with main group III atoms would induce three holes per doped atom and the extent of spin splitting is the largest among these three doped systems. In addition, the induced lattice distortion can suppress spin splitting. Al and Ga dopants induce larger lattice distortion than B dopant does, therefore the ΔE of B-doped MgO is the maximum among main group III atom dopants; however, B-doped MgO is difficult to synthesize experimentally because of its larger formation energy.

3.4. MgO doped with an F atom

As revealed by calculation results for substituting the O atom in MgO with III, IV, V main groups atoms (both metal and non-metal elements) (section 3.1), we find out that the doped

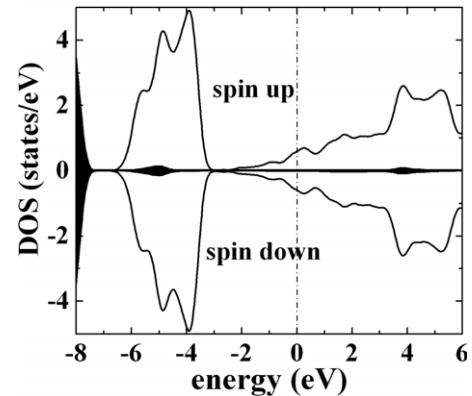


Figure 6. Total DOS (solid) and the projected DOS on the F atom outermost p states (shaded) in F-doped MgO.

MgO systems are all p-type, the doped atom's outermost np orbital energy is higher than that of the O atom, and the systems formed some localized states after doping, therefore they could display half-metal ferromagnetic properties. If the np orbital energy of the dopant atoms is lower than that of the O atom, what is the property of the doped MgO? So we have calculated the F atom doping in MgO using the same method and parameters as previously. The derived DOS is represented in figure 6. The up and down spins are symmetric without polarization and, surprisingly, figure 6 shows that the classical insulator material MgO becomes a conductor after F atom doping. The reasons could be attributed to two facts: (1) one F atom dopant in MgO could introduce one excess electron,

pushing the Fermi level upward, and high doping density could possibly move the Fermi level into the conduction band and reach a degenerate situation; (2) the 2p orbital energy of the F atom is lower than that of the O atom (i.e. more negative in energy), therefore it is impossible for spin splitting to take place near the Fermi level and form the ferromagnetic state. To sum up, for the nonmagnetic atom doped MgO to achieve half-metallic ferromagnetism, the difference of atomic orbital energy between the dopant atoms and the O atom is a key factor. The work of Xia *et al* [22] suggested that the carrier types depend on the difference between the orbital energy of the valence electrons and that of the dopants and the oxygen atoms.

4. Summary

We have systemically studied the electronic structures and the trends of MgO systems doped with III, IV, and V main group atoms at a concentration of 25%. For the first case, all the systems exhibit half-metal ferromagnetic properties (the d electrons have no effect). Besides, we have also derived important conclusions: (1) such p-type doping, regardless of metal or non-metal doping in MgO, displays half-metal ferromagnetic properties as long as the doped atom np orbital energy is lower than that of the O atom and forms localized states after doping; (2) different atomic number of the dopant atoms has little effect on the local magnetic moment for the same main group, whereas different main group dopants strongly affect the magnetic moment; (3) for the doped systems, the trend towards spin splitting is the easiest for B-doped MgO, whereas N-doped MgO is the most stable among them; (4) F-doped MgO does not display half-metal magnetic properties, instead, the system is an electrical conductor. Different doping type leads to dramatic changes of the properties of doped MgO. For the second case, they are all in the paramagnetic ground state and have low formation energy. By contrast with the first case, the derived conclusion is that the ferromagnetism in doped MgO is caused by a hole-mediated magnetic coupling in the np band.

Acknowledgments

This work was supported by the Natural Science Foundation of China (grant No. 10874183), Anhui Provincial Key Laboratory

Special Fund, the Ministry of Science and Technology of China (No. 2005CB623603), Hundred Talent Program of Chinese Academy of Sciences, and the Presidential Scholarship Special Fund.

References

- [1] Elfimov I S, Yunoki S and Sawatzky G A 2002 *Phys. Rev. Lett.* **89** 216403
- [2] Osorio-Guillén J, Lany S, Barabash S V and Zunger A 2006 *Phys. Rev. Lett.* **96** 107203
- [3] Gao F, Hu J F, Yang C L, Zheng Y J, Qin H W, Sun L, Kong X W and Jiang M H 2009 *Solid State Commun.* **149** 855
- [4] Elfimov I S, Rusydi A, Csiszar S I, Hu Z, Hsieh H H, Lin H-J, Chen C T, Liang R and Sawatzky G A 2007 *Phys. Rev. Lett.* **98** 137202
- [5] Kenmochi K, Seike M, Sato K, Yanase A and Katayama-Yoshida H 2004 *Japan. J. Appl. Phys.*, 2 **43** L934
- [6] Gu B, Bulut N, Ziman T and Maekawa S 2009 *Phys. Rev. B* **79** 024407
- [7] Dinh V A, Toyoda M, Sato K and Katayama-Yoshida H 2006 *Phys. Status Solidi c* **3** 4131
- [8] Bannikov V V, Shein I R and Ivanovskii A L 2007 *Tech. Phys. Lett.* **33** 541
- [9] Pardo V and Pickett W E 2008 *Phys. Rev. B* **78** 134427
- [10] Narayan J, Nori S, Pandya D K, Avasthi D K and Smirnov A I 2008 *Appl. Phys. Lett.* **93** 082507
- [11] Ramachandran S and Narayan J 2007 *Appl. Phys. Lett.* **90** 132511
- [12] Dutta P, Seehra M S, Zhang Y and Wender I 2008 *J. Appl. Phys.* **103** 07D104
- [13] Vanderbilt D 1990 *Phys. Rev. B* **41** 7892
- [14] Clark S J, Segall M D, Pickard C J, Hasnip P J, Probert M J, Refson K and Payne M C 2005 *Z. Kristallogr.* **220** 567
- [15] Perdew J P, Burke K and Ernzerhof M 1996 *Phys. Rev. Lett.* **77** 3865
- [16] Anisimov V I, Zaanen J and Andersen O K 1991 *Phys. Rev. B* **44** 943
- [17] Ghijssen J, Tjeng L H, van Elp J, Eskes H, Westerink J, Sawatzky G A and Czyzyk M T 1988 *Phys. Rev. B* **38** 11322
- [18] Monkhorst H J and Pack J D 1976 *Phys. Rev. B* **13** 5188
- [19] Mulliken R S 1955 *J. Chem. Phys.* **23** 1841
- [20] Fei Y 1999 *Am. Miner.* **84** 272
- [21] Whited R C, Flaten C J and Walker W C 1973 *Solid State Commun.* **13** 1903
- [22] Kenmochi K, Dinh V A, Sato K, Yanase A and Katayama-Yoshida H 2004 *J. Phys. Soc. Japan* **73** 2952
- [23] Gai Y Q, Li J B, Li S S, Xia J B and Wei S H 2009 *Phys. Rev. Lett.* **102** 036402
- [24] Mann J B 1967 Atomic structure calculations I. Hartree-Fock energy results for the elements H through Lr *Los Alamos National Laboratory Report LA-3690*